Compatibilization and Toughening of Immiscible Ternary Blends of Polyamide 6, Polypropylene (or a Propylene—Ethylene Copolymer), and Polystyrene

Yan Li,[1] Dong Wang,[2] Jia-Min Zhang,[3] Xu-Ming Xie[1]

[1]*Advanced Materials Laboratory, Department of Chemical Engineering, Tsinghua University, Beijing 100084, China*
[2]*WPI Advanced Institute for Materials Research, Tohoku University, 2-1-1 Katahira, Aoba, Sendai 980-8577, Japan*
[3]*School of Chemistry and Chemical Engineering, Henan Institute of Science and Technology, Xinxiang, Henan 453003, China*

ABSTRACT: In this work, typical ternary blends of three versatile polymers—polyamide 6, a propylene–ethylene copolymer (*co*-PP), and polystyrene—were studied. As a compatibilizer, *co*-PP with randomly dispersed minor ethylene units was multimonomer-melt-grafted in the presence of maleic anhydride, styrene, and dicumyl peroxide. The influence of the ethylene content in *co*-PP and the blend composition on the performance was investigated. Scanning electron microscopy images showed an obvious decrease in the droplet size of the dispersed phase with increases in the compatibilizer content and number of ethylene units in *co*-PP. Peaks of tan δ/temperature curves approaching the glass-transition temperatures of the components were observed with dynamic mechanical thermal analysis. The improved mechanical properties implied good compatibility of the components in the blends. Significant toughening was achieved when the concentration of *co*-PP was increased from 15 to 25 wt %: the elongation at break of the compatibilized blends increased dozens of times in comparison with the elongation at break of the uncompatibilized blends. The introduction of the multimonomer-melt-grafted *co*-PP was shown to be an effective approach for improving immiscible multipolymer blends and to have practical potential. © 2010 Wiley Periodicals, Inc. J Appl Polym Sci 119: 1652–1658, 2011

Key words: blends; compatibilization; mechanical properties

INTRODUCTION

In recent years, more and more attention has been paid to the recycling of plastics. Used plastics are generally in a mixed state. Because polymers are usually immiscible, people have to separate plastics from mixed plastic waste for reuse. However, the separation of plastics is a very hard process. The development of an effective multifunctionalized compatibilizer for multiple-component polymer systems is crucial for the recycling and reuse of plastics.[1–16]

So far, although great progress has been made in polymer blending compatibilization, most studies have been limited to binary polymer blends. Very few researchers have focused on multicomponent polymer blending (not including compatibilizers)[10,12,17–23]

because compatibilizers for multicomponent polymer blends are rarely effective. Some researchers have tried to study the compatibilization of ternary polymer blends with complex compatibilizers. DeBolt and Robertson[10,12] reported an improvement in the compatibility of ternary polymer blends of nylon 66, polystyrene (PS), and polypropylene (PP) with a mixture of an ionomer resin and a styrene-*block*-ethylene-*co*-butylene-*block*-styrene copolymer as a compatibilizer for the system. Groeninckx and co-workers[20,21] reported A/(B/C) ternary polymer blends in which B and C had good compatibility but A and C had some interaction or strong physical effect. They also added maleic anhydride grafted polypropylene (PP-MA) and styrene maleic anhydride copolymer (SMA) to polyamide 6 (PA6)/PP/PS ternary blend systems to form PA6/(PP/PP–MA)/(PS/SMA) and thus improve the interface compatibility.[22] The phase evolution of the blends, which were uncompatibilized or compatibilized with the same compatibilizers, was studied in detail. Investigations also studied the morphology evolution of PP/PS/poly(methyl methacrylate) (PMMA) blends to which PP-*g*-PS graft copolymers of two compositions (55/45 and 70/30), PP-*g*-PMMA, or a styrene-*block*-ethylene-*co*-butylene-*block*-styrene copolymer had been added.[24]

However, the use of complex compatibilizers increases the number of parameters controlling the
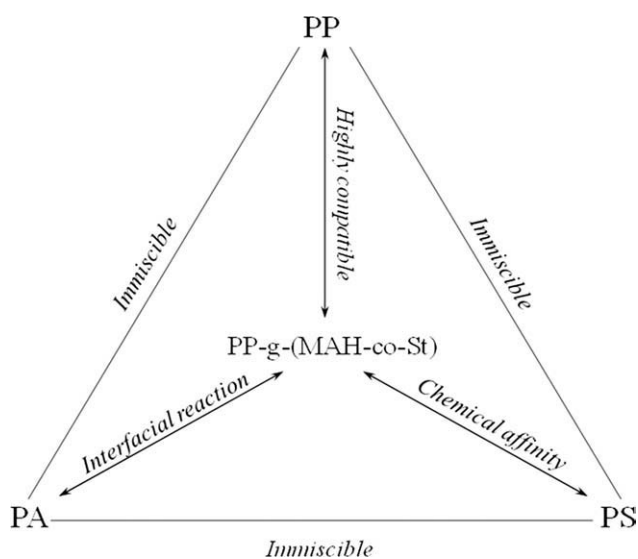
Scheme 1 Schematic representation of the strategy of compatibilization for the PA6/PP/PS ternary blends.

blend morphology, and the process is quite inconvenient because of the complex phase–phase and compatibilizer–compatibilizer interactions.

In our previous work,[25] two monomers, styrene (St) and maleic anhydride (MAH), melt-grafted to PP [PP-g-(St-co-MAH)] were found to be more effective than PP-g-MAH, PP-g-St, and their mixture as a compatibilizer for PP/PA6/PS ternary blends. The addition of PP-g-(MAH-co-St) improved the interface cohesion between the phases of the ternary blends.

Engineering plastics (e.g., PA6 and polycarbonate), polyolefins (e.g., PP and polyethylene), and St polymers (e.g., PS and acrylonitrile butadiene styrene) are versatile polymers composing a great proportion of the plastic market, and most recycled plastic waste comes from these three kinds of polymers. Therefore, it is expected that grafted PP could be used as a multifunctionalized compatibilizer to improve the compatibilization of ternary blends and could be used in the recycling of plastic waste. The mechanism is illustrated in Scheme 1.

In this work, PP and a propylene–ethylene copolymer (co-PP) with randomly dispersed ethylene were melt-grafted to two monomers, MAH and St, to introduce anhydride groups and St segments. The compatibility of the PA6/PP (or co-PP)/PS ternary blends was investigated through the addition of the grafted PP or grafted co-PP. The effects of both the ethylene content in co-PP and the blend composition ratio in the PA6/co-PP/PS ternary systems on the material performance were also studied.

EXPERIMENTAL

Materials

Isotactic PP (H314) and co-PPs [Versify 2000 (V2000), Versify 2200 (V2200), and Versify 2300 (V2300)] with different ethylene contents (5, 9, and 12 wt %) were supplied by Dow Co. The melt flow rate (MFR) index of all PP samples was 2.0 g/10 min (measured according to ASTM D 1238). PA6 (1013B) was obtained from Ube Co. PS (666D) with an MFR of 8.0 g/10 min was procured from Yanshan Petrochemical Co. Both monomers, MAH and St, were products (analytical-grade) of Beijing Chemical Co. (Beijing, China). Dicumyl peroxide (DCP), used as an initiator, was purchased from Beijing Xizhong Chemical Co. (Beijing, China). All the chemicals were used without further purification.

Sample preparation

Compatibilizer preparation

The PP-g-(MAH-co-St) compatibilizers were synthesized by multimonomer melt grafting according to procedures described in the literature.[23,25–29] The monomer and DCP concentrations were set as follows: [MAH] = [St] = 10 [DCP] = 3.0 phr (where phr stands for parts per hundred parts of PP or co-PP). All PP pellets, monomers, and DCP were first mixed and then charged into a single-screw extruder (SH-30, screw diameter = 30 mm, length/diameter = 25, produced by Shanghai Extruder Factory) with a screw rate of 35 rpm. The cylinder temperature was set between 170 and 210°C, and the screw was maintained at 35 rpm. Extrudates were cooled in water, pelletized, and then dried in vacuo at 80°C for 24 h. The unreacted MAH monomers were mostly removed during the drying process.

In this article, unless otherwise specified, g-PP refers to grafted PP or grafted co-PP.

Preparation of the ternary polymer blends

The ternary polymer blends of PA6, PP, and PS were prepared via melt blending with a corotation twin-screw extruder at 120 rpm with a screw diameter of 35 mm and a length/diameter ratio of 48. The temperature profile in the barrel was 200, 210, 220, 230, 240, 240, and 230°C from hopper to die.

Before the blending, all the compositions were dried and used immediately. The pelletized blends were dried and then injection-molded into standard ASTM specimens with a ZT-630 injection-molding machine (Zhejiang Zhenda Equipment Co., Ltd.) for mechanical tests at 240°C.

Analysis and characterization

The grafted PP and co-PP samples were dissolved in refluxing xylene at a concentration of 1% (w/v), and excess acetone was then added to precipitate the grafted and ungrafted PP [i.e., g-PP and PP or co-PP]. After this procedure, the homopolymer, the copolymer of MAH and St, and the unreacted monomers were eliminated. The precipitated samples

TABLE I
Characteristics of the Polyolefins and Grafting Degrees of MAH and St for Corresponding PP (or co-PP)

PP (or co-PP)	Ethylene content (wt %)	MFR for PP (g/10 min)	MFR for g-PP (g/10 min)	R_a for MAH	R_b for St
H314	0	2	9.9	1.91	0.29
V2000	5	2	5.0	2.95	0.36
V2200	9	2	2.8	3.15	0.42
V2300	12	2	1.9	3.78	0.56

The grafting experiments were performed with a single-screw extruder. The monomer and DCP concentrations were set as follows: [MAH] = [St] = 10 [DCP] = 3.0 phr.

were then filtered, washed, and dried *in vacuo* at 80°C for 24 h. The obtained samples were then hot-pressed at 210°C into thin films and were analyzed by Fourier transform infrared (FTIR) with a Nicolet 560 instrument (Nicolet Analytical Instruments, Madison, Wisconsin, USA). The grafting degrees and efficiencies of MAH and St for the purified grafted PP and grafted co-PP are listed in Table I.

Mechanical property measurements were performed at room temperature according to ASTM standards with a crosshead speed of 50 mm/min on a Gotech 2000 universal testing machine (GOTECH Testing Machine, Ind., Taiwan). Five specimens were tested for each kind of blend, and the average value was obtained. The Izod notched impact strength of the materials was measured with an XJUD-5.5 impact-testing machine (Chengde JinJian Testing Instrument Co., Ltd, China). The average of at least seven measurements for each sample was obtained.

The morphologies of the blends were examined with an S-450 scanning electron microscope (Hitachi, Japan). Fracture surfaces of impact-fractured sections were examined. Each sample was gold-coated with a film thickness of 20 nm in a sputtering coater before the scanning. The accelerating voltage was 20 kV.
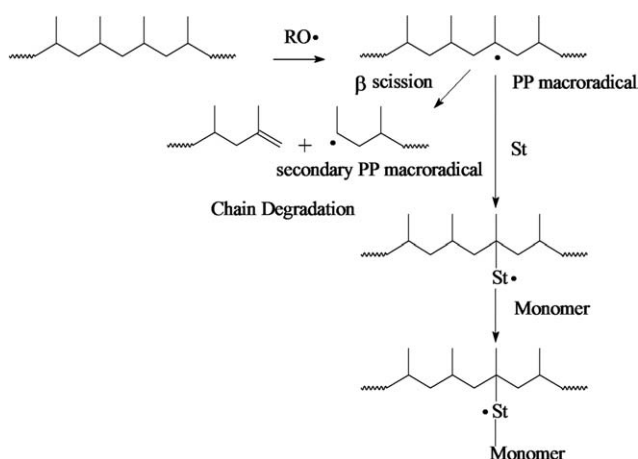
The melting and crystallization behaviors of the compatibilized and uncompatibilized blends were determined on a differential scanning calorimeter (DSC) (Shimadzu, DSC-60, Japan). Samples (3–5 mg) were sealed in an aluminum pan and used under a nitrogen atmosphere. The samples were first heated to 270°C at a heating rate of 20°C/min, maintained at this temperature for 5 min, and then cooled to 50°C at a rate of 10°C/min. For the determination of the melting behavior, they were reheated at a rate of 10°C/min.

Dynamic mechanical thermal analysis (DMTA) of the blends was carried out with a TA 2980 apparatus (TA Instruments, New Castle, Delaware, USA). Test data were collected from −70 and 150°C at a frequency of 1 Hz and at a scanning rate of 5°C/min.

RESULTS AND DISCUSSION

FTIR spectroscopy

During the grafting process, the monomer St, as mentioned elsewhere,[26,27] was adopted as the stabilizer for the PP macroradicals so that more stable radicals (St macroradicals) could be formed; these assisted functional monomer such as MAH and glycidyl methacrylate, which were grafted to a great extent onto the PP backbone (Scheme 2). After melt grafting in the single-screw extruder, all the grafted PP samples were purified to characterize the monomer graft ratios by FTIR. Figure 1 shows FTIR spectra of the grafted PP and grafted co-PP. The band at 702 cm^{-1} represents monosubstituted benzene, and the bands at 1782 and 1857 cm^{-1} are attributed to the stretching vibration of the carbonyl group for the grafted anhydride unit, which can be found in all modified PPs; this implies that the monomers were grafted onto PP skeletons.

The absorption band at 2723 cm^{-1} can be chosen as an internal reference in this case.[25,27,30] The absorbance ratio of the areas of the bands at 1782 and

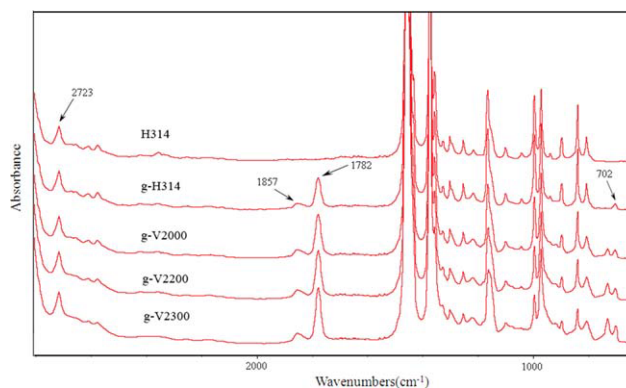**Scheme 2** Schematic representation of the graft reactions of PP.

Figure 1 FTIR spectra of grafted PP and grafted co-PP. [Color figure can be viewed in the online issue, which is available at wileyonlinelibrary.com.]
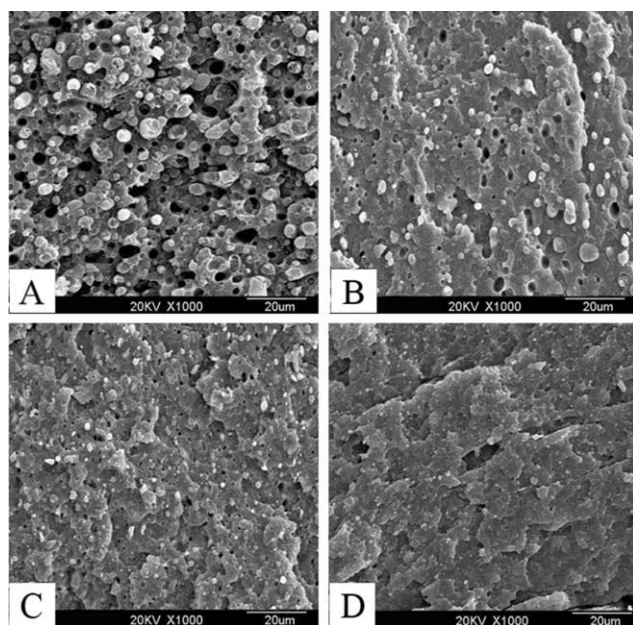
Figure 2 SEM micrographs of impact-fracture surfaces of PA6/V2000 + g-V2000/PS (w/w) blends with different composition ratios: (A) 60/20 + 0/20, (B) 60/15 + 5/20, (C) 60/10 + 10/20, and (D) 60/0 + 20/20.

2723 cm^{-1} (R_a) shows the relative grafting degree of MAH. Similarly, the absorbance ratio of the areas of the bands at 702 and 2723 cm^{-1} (R_b) represents the relative grafting degree of St.

The spectra indicate that the grafting degree increased with the ethylene content increasing in co-PP, as listed in Table I.

Randomly dispersed ethylene units in co-PP restricted the crystallization of co-PP: the greater the ethylene content, the lower the crystallinity of co-PP. As is known, the amorphous part could absorb a larger amount of the monomer for co-PP with a higher ethylene content, and this led to more contact between the monomers and PP chains during the grafting reaction and a higher grafting degree of co-PP.

Table I also shows that the MFR value of g-PP decreased with the ethylene content increasing in co-PP. This means that α-H on the PP backbone was easily abstracted to produce the PP macroradical. The PP macroradical was not stable, so the secondary PP macroradical was generated continuously and rapidly (i.e., β scission). Although β scission was not a termination reaction and produced an equivalent of secondary PP radicals, the termination rate of secondary PP radicals was relatively rapid.[31] Consequently, the number and lifetime of the radicals were largely reduced for neat PP, and this implied that the lower the ethylene content in co-PP was, the higher the MFR value of co-PP was during melt grafting. There were more tertiary carbon atoms where β scission usually occurred in neat PP versus co-PP. The addition of the St monomer could

prevent β scission of the PP backbone and lead to an enhancement of the grafting degree of co-PP versus homo-PP. The less β scission there was, the higher the grafting degree of co-PP was.

Scanning electron microscopy (SEM)

Figure 2 shows SEM micrographs of impact-fractured surfaces of PA6/V2000 + g-V2000/PS blends with different compatibilizer contents. Figure 2(A) reveals that all the particles debonded from the matrix were clearly loose on the fractured surface. As shown in Figure 2(B–D), the size of the dispersed phase in the PA6
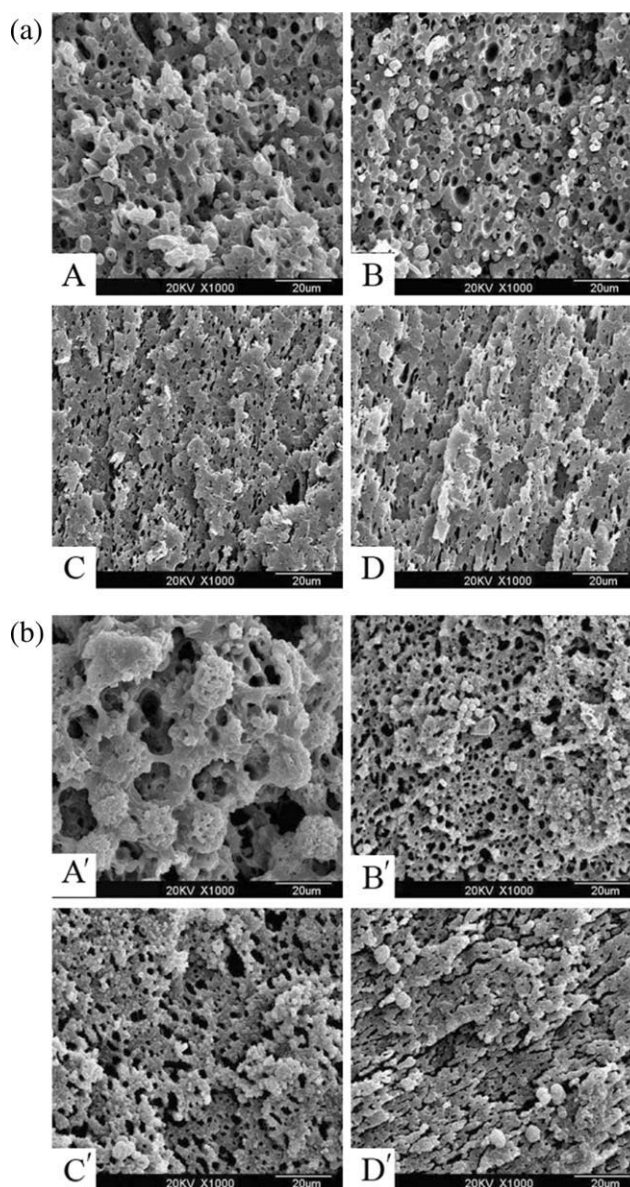

Figure 3 SEM micrographs of impact-fractured surfaces of etched PA6/V2000 + g-V2000/PS (W/W/W) blends with composition ratios of (A,A′) 60/20 + 0/20, (B,B′) 60/15 + 5/20, (C,C′) 60/10 + 10/20, and (D,D′) 60/0 + 20/20: (a) blends etched with THF (for PS) and (b) blends etched with xylene (for PS and PP).
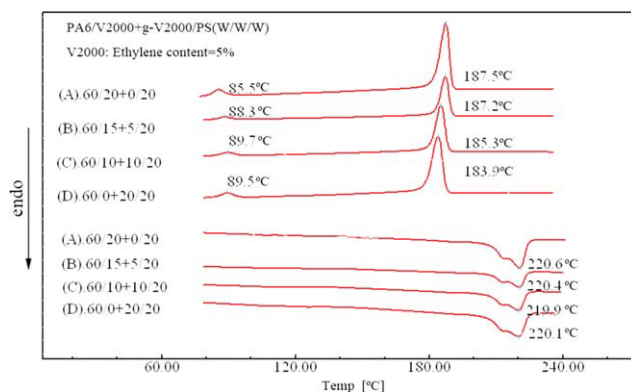
Figure 4 DSC curves of PA6/V2000 + *g*-V2000/PS blends with different compatibilizer contents. [Color figure can be viewed in the online issue, which is available at wileyonlinelibrary.com.]

matrix decreased with the compatibilizer content increasing, and fewer debonded particles could be observed.

Micrographs of the PS phase extracted by tetrahydrofuran (THF) in the blends are shown in Figure 3(A–D), whereas the morphologies of PS and V2000 (*co*-PP) dispersed phases extracted by xylene are presented in Figure 3(A′–D′). After PS phase extraction, the hole size decreased with increasing compatibilizer content, as shown in Figure 3(A–D). A similar phenomenon was observed after the PS and V2000 phases were extracted, as shown in Figure 3(A′–D′). For compatibilized blends, as presented in Figures 2(B–D) and 3(B–D,B′–D′), the V2000 and PS phases in the matrix were very uniform and small (even 0.5 μm for the blend system with 20 wt % compatibilizer), and this indicated that the interfacial adhesion between the dispersed phases and the matrix was improved.

In the systems of uncompatibilized PA6/PP (or *co*-PP)/PS blends, interfaces between different phases lacked adhesion and exhibited characteristics typical of brittle fracture [Figs. 2(A) and 3(A,A′). The compatibilizers (*g*-PP) with anhydride-functional groups and St segments could react with amino groups in
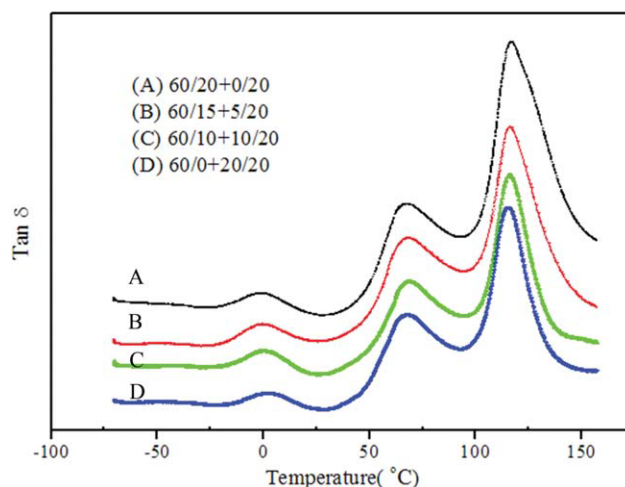

Figure 5 Tan δ as a function of temperature for PA6/V2000 + *g*-V2000/PS blends with different compatibilizer contents. [Color figure can be viewed in the online issue, which is available at wileyonlinelibrary.com.]

PA6 at the interface via chemical reactions and had an intermolecular attraction or affinity to PS as well. Therefore, the addition of *g*-PP could effectively improve the interface adhesion between the phases and result in good compatibility of the PA6/PP (or *co*-PP)/PS blends.

Thermal properties

Figure 4 shows the differential scanning calorimetry (DSC) curves of PA6/V2000 + *g*-V2000/PS blends with different *g*-V2000 contents. The crystallization temperature of PA6 slightly decreased with increasing compatibilizer content, whereas that of V2000 shifted to a higher temperature. This indicated that the grafted polymer acted as a nucleating agent and improved the crystallization behavior of V2000, and the crystallization behavior of PA6 chains was restricted because of the graft reaction between PA6

TABLE II
Thermal Properties of PA6/V2000 + *g*-V2000/PS Blends with Different Composition Ratios and an Ethylene Concentration of 5 wt %

	PA6/V2000 + *g*-V2000/PS (w/w)			
	60/20 + 0/20	60/15 + 5/20	60/10 + 10/20	60/0 + 20/20
T_c (°C) of V2000 in the blends[a]	85.5	88.3	89.7	89.5
T_c (°C) of PA6 in the blends[a]	187.5	187.2	185.3	183.9
T_m (°C) of PA6 in the blends[a]	220.6	220.4	219.9	220.1
T_g (°C) of V2000 in the blends[b]	−1.3	0.2	0.6	2.2
T_g (°C) of PA6 in the blends[b]	68.6	68.4	68.4	67.7
T_g (°C) of PS in the blends[b]	117.1	116.5	116.1	115.3

T_c = crystallization temperature; T_g = glass-transition temperature; T_m = melting temperature.
[a] Examined by DSC.
[b] Examined by DMTA.

TABLE III
Mechanical Properties of PA6/V2000 + g-V2000/PS Blends with Different Compatibilizer Concentrations and an Ethylene Concentration of 5 wt %

Blend (w/w)	Tensile strength (MPa)	Elongation (%)	Impact strength (J/m)	MFR (g/10 min)
60/20 + 0/20	45.2 ± 0.2	4.3 ± 1.4	13.9 ± 1.1	27.3
60/15 + 5/20	45.9 ± 0.2	13.5 ± 2.1	14.8 ± 1.4	17.8
60/10 + 10/20	46.4 ± 0.3	16.2 ± 3.3	17.9 ± 1.3	8.1
60/0 + 20/20	45.4 ± 0.2	21.3 ± 3.1	22.5 ± 2.0	3.2

and g-PP during blending. The results were similar to those found for the crystallization behavior of PA6 in PP/PA6 blends.[32] This also demonstrated that the addition of the compatibilizers improved interactions between the phases. No clear melting temperature for V2000 was observed, and no clear change in the melting temperature of the PA6 component in the blends was detected. The data for the glass-transition and melting temperatures of the blends are summarized in Table II.

Figure 5 demonstrates tan δ as a function of temperature for PA6/V2000 + g-V2000/PS blends with different compatibilizer contents. The three peaks of each curve (from a low temperature to a high temperature) represent the glass-transition temperatures of V2000, PA6, and PS, and those data are presented in Table II. Generally, the glass-transition temperatures of the components in the blends with partial compatibility tended to shift toward one another. The glass-transition temperatures of PA6, PS, and V2000 in the blends indeed approached one another when the concentration of the compatibilizers in the blends increased from 0 to 20 wt %. This result was consistent with the SEM and DSC analysis and implied improved compatibility with increasing g-PP content.

Mechanical properties

The mechanical properties of PA6/V2000 + g-V2000/PS (60/20/20) blends with different compatibilizer contents are presented in Table III. With increasing compatibilizer content, the mechanical properties of the blends continuously improved (especially the elongation at break and impact strength), whereas no obvious change occurred in the tensile strength. The improvement in the mechanical properties indicated that g-PP was indeed an effective compatibilizer for the compatibilization of the phases of the blends. This result was consistent with the aforementioned results of SEM, DSC, and DMTA.

Table IV summarizes the mechanical properties of PA6/PP (or co-PP)/PS blends with different ethylene contents in co-PP prepared by twin-screw extrusion.

For uncompatibilized PA6/PP (or co-PP)/PS blends, the tensile strength decreased with increasing ethylene content in co-PP, and the values of the Izod impact strength and elongation at break were relatively low, although they were slightly amplified with increasing ethylene content in co-PP.

The enhancement of the mechanical properties was obvious for the compatibilized systems with the addition of 5 wt % g-PP because of the better compatibility between the phases. The elongation at break and impact strength of PA6/V2300 + g-PP/PS (60/15 + 5/20) blends were more than twice those of the PA6/H314 + g-PP/PS system, with only the disadvantage of an approximately 20% decrease in the tensile strength when V2300 was used instead of H314 in the blends. The remarkable enhancement of both the toughness and ductility of the PA6/PP (or co-PP) + g-PP/PS (60/15 + 5/20) blends was mainly due to the increasing ethylene content in co-PP.

TABLE IV
Mechanical Properties of PA6/PP (or co-PP)/PS Blends with Different Compositions with or without Compatibilizers

Blend (w/w)	Tensile strength (MPa)	Elongation (%)	Impact strength (J/m)	MFR (g/10 min)
PA6/H314/PS (60/20/20)	46.9 ± 0.3	3.4 ± 0.9	13.5 ± 0.6	36.7
PA6/V2000/PS (60/20/20)	45.2 ± 0.2	4.3 ± 1.4	13.9 ± 1.1	27.3
PA6/V2200/PS (60/20/20)	40.0 ± 0.3	5.7 ± 1.7	16.6 ± 1.3	31.1
PA6/V2300/PS (60/20/20)	38.8 ± 0.2	6.6 ± 1.9	18.3 ± 1.6	29.6
PA6/H314 + g-H314/PS (60/15 + 5/20)	50.4 ± 0.3	8.4 ± 2.8	14.7 ± 0.9	19.3
PA6/V2000 + g-V2000/PS (60/15 + 5/20)	45.9 ± 0.2	13.5 ± 2.1	14.8 ± 1.4	17.8
PA6/V2200 + g-V2200/PS (60/15 + 5/20)	40.5 ± 0.3	19.6 ± 3.1	34.3 ± 2.4	17.7
PA6/V2300 + g-V2300/PS (60/15 + 5/20)	40.4 ± 0.2	20.3 ± 5.2	34.7 ± 2.9	21.8
PA6/H314/PS (60/30/10)	41.6 ± 0.4	6.6 ± 1.8	15.5 ± 2.0	28.7
PA6/V2000/PS (60/30/10)	34.4 ± 0.2	7.2 ± 2.1	15.7 ± 1.8	28.8
PA6/V2200/PS (60/30/10)	32.9 ± 0.3	8.9 ± 1.7	25.6 ± 2.1	28.9
PA6/V2300/PS (60/30/10)	31.2 ± 0.2	9.7 ± 2.3	28.0 ± 2.3	28.1
PA6/H314 + g-H314/PS (60/25 + 5/10)	46.2 ± 0.4	64.1 ± 11.2	27.5 ± 3.1	8.4
PA6/V2000 + g-V2000/PS (60/25 + 5/10)	36.8 ± 0.1	187.8 ± 33.7	31.0 ± 2.9	8.6
PA6/V2200 + g-V2200/PS (60/25 + 5/10)	34.8 ± 0.3	261.0 ± 37.3	53.3 ± 4.4	8.5
PA6/V2300 + g-V2300/PS (60/25 + 5/10)	33.8 ± 0.2	263.0 ± 41.2	115.1 ± 6.2	8.7

When the concentration of *co*-PP increased from 20 to 30 wt % and the concentration of PS decreased from 20 to 10 wt % in the blends, the mechanical properties of the uncompatibilized PA6/PP/PS (60/30/10) blends were also quite weak. For PA6/PP (or *co*-PP) + *g*-PP/PS blends with the composition ratio of 60/25 + 5/10, the mechanical properties were greatly improved (especially the elongation at break and impact strength) with increasing ethylene content in *co*-PP. Moreover, the elongation at break and impact strength of PA6/V2300 + *g*-V2300/PS (60/25 + 5/10) blends were increased several times versus those of PA6/H314 + *g*-H314/PS (60/25 + 5/10) blends. Meanwhile, the loss of the tensile strength was 25% with V2300 instead of H314. These results were also confirmed by the effect of toughening PA6 with *g*-V2300.[23]

CONCLUSIONS

Immiscible ternary blends of PA6, PP (or *co*-PP), and PS were effectively compatibilized by the addition of *g*-PP prepared by multimonomer melt grafting. With increasing *g*-PP content, both the PP (or *co*-PP) and PS phases in the PA6 matrix were dispersed uniformly and finely, with even a 0.5-μm diameter for the blend system with 20 wt % compatibilizer, and this implies that multimonomer-melt-grafted PP-*g*-(MAH-*co*-St) is an effective compatibilizer for multicomponent blend systems.

The toughness of the blends was greatly improved by changes in the content of ethylene in *co*-PP (from V2000 to V2300), with only the disadvantage of an approximately 20% decrease in the tensile strength. Furthermore, when the PA6 concentration was fixed at 60 wt % and the *co*-PP content was changed from 15 to 25 wt % in the compatibilized blends, the mechanical properties (especially the elongation at break and impact strength) were significantly enhanced. Toughened multicomponent blend systems with balanced mechanical properties were achieved.

References

1. Alsewailem, F. D.; Gupta, R. K. Int Polym Process 2006, 21, 189.
2. Fang, Z. P.; Zeng, M. F.; Cai, G. P.; Xu, C. W. J Appl Polym Sci 2001, 82, 2947.
3. Mehrabzadeh, M.; Farahmand, F. J Appl Polym Sci 2001, 80, 2573.
4. Phuong, N. T.; Gilbert, V.; Chuong, B. J Reinforced Plast Compos 2008, 27, 1983.
5. Arena, U.; Mastellone, M. L.; Perugini, F. Int J Life Cycle Assess 2003, 8, 92.
6. Petra, P.; Paul, D. R. Polym Rev 2003, 43, 87.
7. Ha, C.-S.; Park, H.-D.; Cho, W.-J. J Appl Polym Sci 2000, 76, 1048.
8. Kim, G. H.; Hwang, S. S.; Cho, B. G.; Hong, S. M. Macromol Symp 2007, 249, 485.
9. Hyun, D. C.; Jeong, U.; Ryu, D. Y. J Polym Sci Part B: Polym Phys 2007, 45, 2729.
10. DeBolt, M. A.; Robertson, R. E. Polym Eng Sci 2006, 46, 385.
11. Hong, S. M.; Hwang, S. S.; Jeon, B. H.; Choi, J. S.; Kim, H. B.; Lim, S. T.; Choi, H. J. J Mater Sci 2005, 40, 3857.
12. DeBolt, M. A.; Robertson, R. E. Polym Eng Sci 2004, 44, 1800.
13. Washburn, N. R.; Lodgemothy, T. P.; Bates, F. S. J Phys Chem B 2000, 104, 6987.
14. Valera, T. S.; Morita, A. T.; Demarquette, N. R. Macromolecules 2006, 39, 2663.
15. Rybnicek, J.; Lach, R.; Lapcikova, M.; Steidl, J.; Krulis, Z.; Grellmann, W.; Slouf, M. J Appl Polym Sci 2008, 109, 3210.
16. Hachiya, H.; Takayama, S.; Takeda, K. J Appl Polym Sci 1998, 70, 2515.
17. Moussaif, N.; Jerome, R. Polymer 1999, 40, 3919.
18. Guo, H. F.; Packirisamy, S.; Gvozdic, N. V.; Meier, D. J. Polymer 1997, 38, 785.
19. Guo, H. F.; Packirisamy, S.; Gvozdic, N. V.; Meier, D. J. Polymer 1997, 38, 4915.
20. Dedecker, K.; Groeninckx, G. Polymer 1998, 39, 4985.
21. Everaerta, V.; Groeninckx, G.; Aerts, L. Polymer 2000, 41, 1409.
22. Omonov, T. S.; Harrats, C.; Groeninckx, G. Polymer 2005, 46, 12322.
23. Zhang, J. M.; Yan, L.; Xie, X. M. Acta Polym Sinica 2009, 4, 381.
24. Freitas, C. A.; Valera, T. S.; Souza, A. M. C.; Demarquette, N. R. Macromol Symp 2007, 247, 260.
25. Wang, D.; Xie, X. M. Polymer 2006, 47, 7859.
26. Xie, X. M.; Chen, N. H.; Guo, B. H.; Li, S. Polym Int 2000, 49, 1677.
27. Li, Y.; Xie, X. M.; Guo, B. H. Polymer 2001, 42, 3419.
28. Li, Z. J.; Xie, X. M.; Guo, B. H. Chem J Chin Univ 2004, 25, 1941.
29. Li, Z. J.; Guo, B. H.; Hu, P.; Xie, X. M. Chem J Chin Univ 2001, 22, 1244.
30. Wang, D.; Xie, X. M.; Jow, J.; Chen, H. Y.; Lai, S. Y. J Appl Polym Sci 2008, 108, 1737.
31. Machado, A. V.; Covas, J. A.; Duin, M. V. Polymer 2001, 42, 3649.
32. Zhang, J. C.; Xie, X. M.; Guo, B. H. Acta Polym Sinica 2002, 3, 282.